



## **Dataset of non-crimp fabric reinforced composites for an X-ray computer tomography aided engineering process**

Downloaded from: <https://research.chalmers.se>, 2021-08-31 12:04 UTC

Citation for the original published paper (version of record):

Auenhammer, R., Mikkelsen, L., Asp, L. et al (2020)

Dataset of non-crimp fabric reinforced composites for an X-ray computer tomography aided engineering process

Data in Brief, 33

<http://dx.doi.org/10.1016/j.dib.2020.106518>

N.B. When citing this work, cite the original published paper.



## Data Article

# Dataset of non-crimp fabric reinforced composites for an X-ray computer tomography aided engineering process



Robert M. Auenhammer<sup>a,b,\*</sup>, Lars P. Mikkelsen<sup>b</sup>, Leif E. Asp<sup>a</sup>,  
Brina J. Blinzler<sup>a</sup>

<sup>a</sup> Industrial and Materials Science, Chalmers University of Technology, SE-41296 Göteborg, Sweden

<sup>b</sup> Composite Materials, DTU Wind Energy, Technical University of Denmark, DK-4000 Roskilde, Denmark

## ARTICLE INFO

*Article history:*

Received 20 October 2020

Revised 5 November 2020

Accepted 6 November 2020

Available online 10 November 2020

*Keywords:*

Composites

X-ray computer tomography

Segmentation

Finite element modelling

## ABSTRACT

This data in brief article describes a dataset used for an X-ray computer tomography aided engineering process consisting of X-ray computer tomography data and finite element models of non-crimp fabric glass fibre reinforced composites. Additional scanning electron microscope images are provided for the validation of the fibre volume fraction. The specimens consist of 4 layers of unidirectional bundles each supported by off-axis backing bundles with an average orientation on  $\pm 80^\circ$ . The finite element models, which were created solely on the image data, simulate the tensile stiffness of the samples. The data can be used as a benchmark dataset to apply different segmentation algorithms on the X-ray computer tomography data. It can be further used to run the models using different finite element solvers.

© 2020 The Authors. Published by Elsevier Inc.

This is an open access article under the CC BY-NC-ND license (<http://creativecommons.org/licenses/by-nc-nd/4.0/>)

DOI of original article: [10.1016/j.compstruct.2020.113136](https://doi.org/10.1016/j.compstruct.2020.113136)

\* Corresponding author.

E-mail address: [robaue@chalmers.se](mailto:robaue@chalmers.se) (R.M. Auenhammer).

<https://doi.org/10.1016/j.dib.2020.106518>

2352-3409/© 2020 The Authors. Published by Elsevier Inc. This is an open access article under the CC BY-NC-ND license (<http://creativecommons.org/licenses/by-nc-nd/4.0/>)

## Specifications Table

Subject	Material Science
Specific subject area	Non-crimp reinforced composites, image based numerical analysis
Type of data	Image: <i>X-ray tomography data, Scanning electron microscopy</i> Numerical model: <i>Finite element model</i>
How data were acquired	Laboratory X-ray tomography scanner (Zeiss Xradia 520 Versa) Laboratory Scanning electron microscope (VEGA3 SBU) Finite element model for the commercial solver Abaqus™ created in the pre-processor Ansa™
Data format	Raw: Reconstructed X-ray computer tomography image data as .nii-file, Scanning electron microscope images as .tif-file Numerical model: Abaqus™ model as .inp-file
Parameters for data collection	Non-crimp glass-fibre reinforced specimens containing unidirectional bundles with off-axis backing bundles with an angle of $\pm 80^\circ$
Description of data collection	Three specimens have been scanned consisting of three single scans each that have been stitched together with a resolution of $10.9\ \mu\text{m}$ and $5.47\ \mu\text{m}$ , respectively. The scanning electron microscope images have been used to validate the fibre volume fraction inside the fibre bundles. The finite element models combine an elementwise material orientation with an orthotropic material model.
Data source location	Roskilde, Denmark, Latitude: 55.695343, Longitude: 12.08921
Data accessibility	The data is available online at: Automated X-ray computer tomography segmentation method for finite element analysis of non-crimp fabrics reinforced composites <a href="https://doi.org/10.5281/zenodo.3830790">https://doi.org/10.5281/zenodo.3830790</a>
Related research article	R. M. Auenhammer, L. P. Mikkelsen, L. E. Asp, B. J. Blinzler, Automated X-ray computer tomography segmentation method for finite element analysis of non-crimp fabric reinforced composites, <i>Composite Structures</i> 256 (2021) 113136, doi: <a href="https://doi.org/10.1016/j.compstruct.2020.113136">https://doi.org/10.1016/j.compstruct.2020.113136</a>

## Value of the Data

- The dataset contains high quality reconstructed X-ray computer tomography data of a non-crimp fabric reinforced composite. This data can be used for various applications.
- The image data can be used to work with or change the segmentation algorithm described in [1].
- The data contains finite element models for the commercial solver Abaqus™. They can be easily changed to other solvers like LS-Dyna™.
- The finite element models can be used to apply different material models or run different load cases.
- The dataset can be used to analyse the high-resolution scanning electron microscope images of non-crimp fabric reinforced composites.
- The dataset can be used for validation of the observations and conclusions reported in [2].

## 1. Data Description

The presented data consists of three reconstructed X-ray computer tomography scans of non-crimp fabric reinforced glass fibre composites (Fig. 1). The scans were taken with Zeiss Xradia 520 Versa at DTU Roskilde, Denmark. The image data for all three scans is saved and uploaded as .nii-file. Each scan consists of three single scans that were stitched together in order to increase the field of view. For the acquisition a detector with  $2000 \times 2000$  pixel was used. Different settings for the accelerating voltage, power, exposure time, number of projections and binning were chosen. A full rotation of the sample was performed and the optical magnification as well

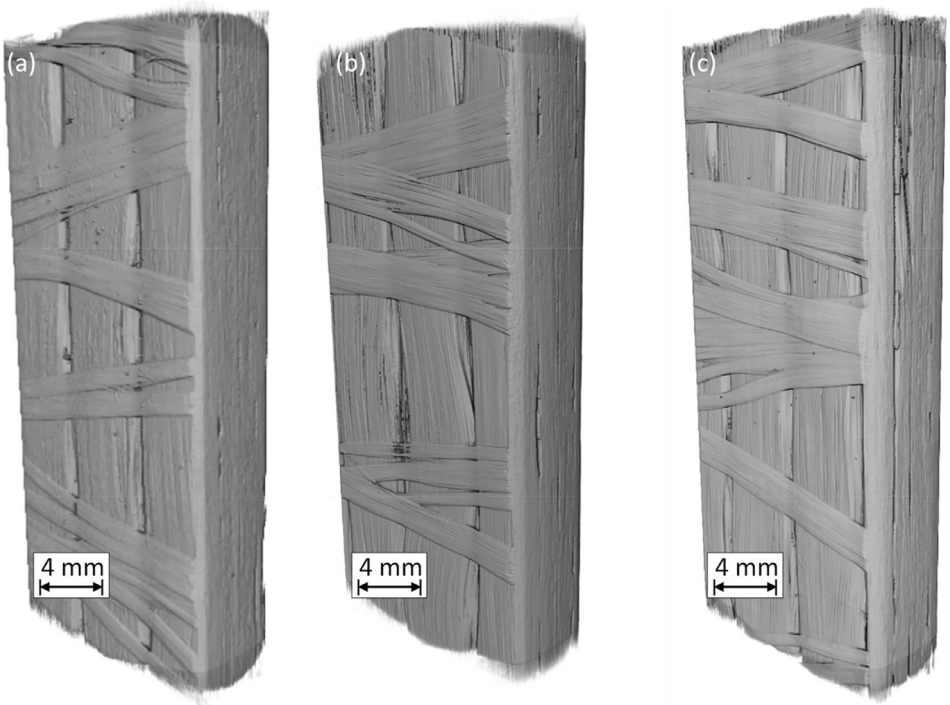


**Fig. 1.** Reconstructed X-ray computer tomography images of Sample-A (a), Sample-G (b) and Sample-E (c) scanned at DTU Roskilde, Denmark with a Zeiss Xradia 520 Versa. The data is visualised with a volume rendering. At the top and bottom beam cone effects become visible. The parts with beam cone effects were removed for the image processing.

**Table 1**

X-ray computer tomography acquisition and reconstruction settings for a Zeiss Xradia 520 Versa at DTU Roskilde, Denmark. All three scans consist of three single scans that have been stitched together.

Parameter	Sample-A	Sample-E	Sample-G
Accelerating Voltage [kV]	50	50	40
Power [W]	4.0	4.0	3.0
Optical magnification	0.4x	0.4x	0.4x
Source to sample distance [mm]	21	21	21
Detector to sample distance [mm]	110	110	110
Exposure time [s]	4	16	12
No. of projections	3601	4501	5801
Rotation	360°	360°	360°
Binning	2	1	2
Pixel size [ $\mu\text{m}$ ]	10.9	5.47	10.9
Number of single stitches	3	3	3
Total scanning time [h]	21	72	66
Cropped file-size [GB]	1.6	12.6	1.6

as the distance sample to source and sample to detector were kept constant. Further details can be found in [Table 1](#). For each scan a .pdf-file with settings from the scanner is uploaded.

Additionally, scanning electron microscope images are described ([Fig. 2](#)). The novel segmentation approach for non-crimp reinforced composites in [\[1\]](#) can be used to calculate the fibre volume fraction based on the fibre areal weight. To validate the accuracy of the determined fibre volume fraction of this new approach scanning electron microscope images were acquired using a TESCAN VEGA3 SEM at DTU Roskilde. Therefore, the samples, which were first scanned

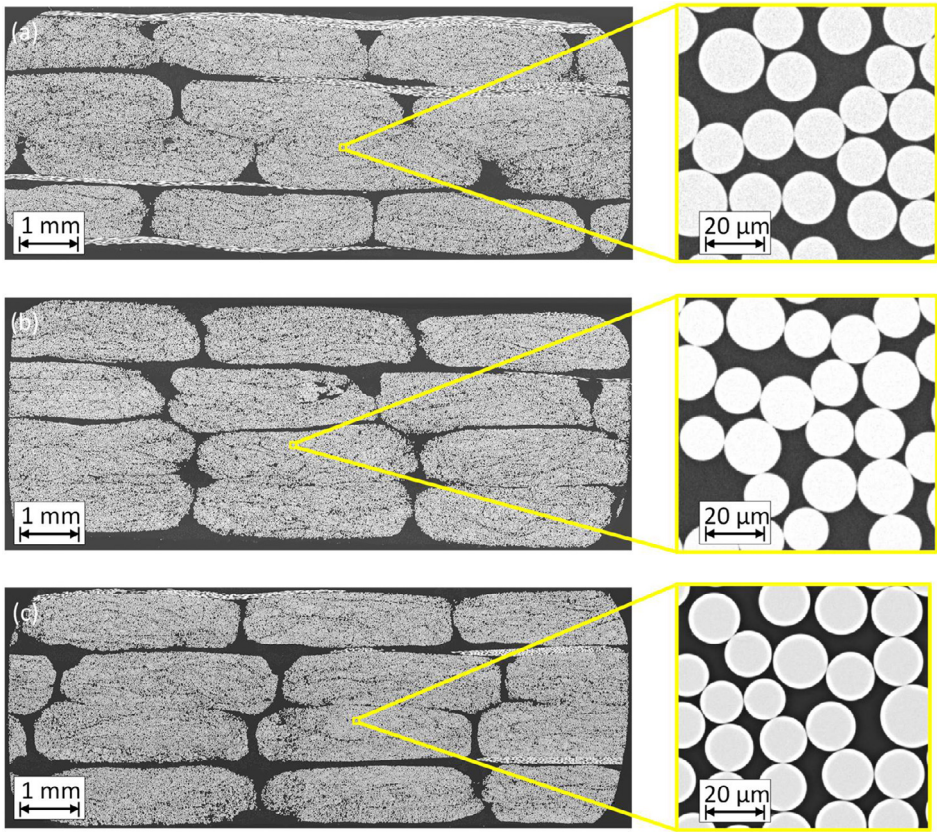


**Fig. 2.** Scanning electron microscope images of Sample-A (a), Sample-G (b) and Sample-E (c) scanned at DTU Roskilde, Denmark with a VEGA3 SBU. With a pixel size of 250–350 nm the fibre diameter will cover 50–70 pixels.

by tomography, were cut in half. The cutting surface was polished and an approximately 10 nm thin layer of carbon was applied on the surface using a Bal-Tec SCD 005 Sputter Coater. The SEM images were acquired using a solid-state backscattered detector, an accelerating voltage of 20 kV and a magnification that resulted in a pixel size of 346.02 nm, 349.65 nm and 253.80 nm for sample A, E and G, respectively. The data is uploaded as .tif-files. In addition, a meta-file with acquisition details is attached.

Furthermore, the final finite element models for all three samples are presented (Fig. 3). As solver the commercial code Abaqus™ was used. All three models consist of a main file (.inp-file), that defines the material model, the load case and output data, and a mesh file (.inp-file). The mesh file is called in the main deck via an *\*INCLUDE* command.

## 2. Experimental Design, Materials and Methods

The non-crimp reinforced glass fibre composite is laid up of four unidirectional bundles stitched together by a thread. Additionally, randomly placed overlapping backing bundles are supporting the structure. The backing bundles are orientated at approximately  $\pm 80^\circ$  which results in a stacking sequence [b/0,b/0]<sub>s</sub>, where “b” denotes a layer of backing bundles and “0” a layer of unidirectional bundles. The reader is referred to [3] for a detailed description of how the samples were manufactured and to [4] for a how the samples were milled.



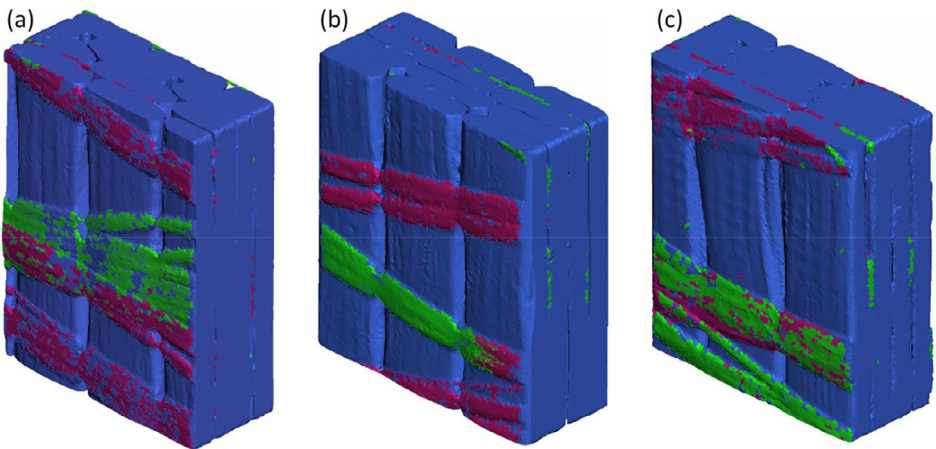


**Fig. 3.** Finite element models of Sample-A (a), Sample-G (b) and Sample-E (c) based on the X-ray computer tomography image data. The surrounding matrix is masked.

The scanning electron microscope images were processed with a Matlab script, where the data was loaded with the function *imread* and binarized with the function *imbinarize*. Therefore, the “adaptive” option was chosen. With the function *imcrop* single bundles can be cropped chosen, in order to focus only on the fibre volume fraction inside bundles. The function *imhist* returns the number of pixels of both components. Those were used to calculate the fibre volume fraction inside the fibre bundles.

The mesh for all three models has been created based on the segmentation outcome described in [1]. This surface mesh, as segmentation outcome, most likely consists of a huge number of elements; around 5 million for this study. A reduction of this element number is crucial to obtain finally a reasonable number of solid elements. This reduction of the surface elements most likely leads to intersections and element quality issues e.g. high aspect ratios. Some experience is required for this process. A fully automated way would however suffer from larger inaccuracies in the surface representation. The average element size was set to 120  $\mu\text{m}$ .

With a pre-processed surface mesh of the fibre bundle, the matrix mesh surrounding the bundles could be generated. Therefore, a block of the size of the scanned data was created and applied with a 2D surface mesh. The fibre bundle elements that coincided with the matrix elements were projected onto the matrix surface and the nodes were pasted on each other. By this procedure a closed volume for the matrix surrounding the fibre bundles could be generated. In the end, penetration-free 3D solid meshes for both components (matrix and bundles) were obtained.

In the mesh file all elements that belong to a fibre bundle are assigned with their material orientation with the Abaqus keywords \*ORIENTATION, \*DISTRIBUTION TABLE and \*DISTRIBUTION. Further details about those keywords can be found in the Abaqus Keywords Reference Guide (Note: Not publicly available).

A linear orthotropic material model was defined. The parameters were calculated with a micro-mechanical model based on the fibre volume fraction inside the bundles. Further details about the material model can be found in [1]. The values in the material model are normalised with the single fibre stiffness used in the unidirectional bundles.

### CRediT Author Statement

*Robert M. Auenhammer*: Methodology, Software, Validation, Visualization, Writing - Original Draft, Writing - Review & Editing

*Lars P. Mikkelsen:* Conceptualization, Funding acquisition, Resources, Supervision, Validation, Writing -Review & Editing,

*Leif E. Asp:* Funding acquisition, Supervision, Validation, Writing - review & editing

*Brina J. Blinzler:* Funding acquisition, Supervision, Validation, Writing - review & editing

## Declaration of Competing Interest

The authors declare that they have no known competing financial interests or personal relationships which have or could be perceived to have influenced the work reported in this article.

## Acknowledgements

This study was funded by EU [Horizon 2020](#) Marie Skłodowska-Curie Actions Innovative Training Network: MULTiscale, Multimodal and Multidimensional imaging for EngineerRING (MUM-MERING), Grant Number [765604](#) and the Erna and Victor Hasselblad foundation grant for female scientists. Financial support from VINNOVA (the Swedish Innovation Agency) via LIGHTer Academy is also gratefully acknowledged. The X-Ray computer tomography data was acquired using the Zeiss Xradia 520 Versa from the DTU ([Technical University of Denmark](#)) Centre for Advanced Structural and Material Testing (CAS-MAT), grant no. [VKR023193](#) from Villum Fonden. At DTU in Roskilde the scanning electron microscopy images were taken.

## References

- [1] R.M. Auenhammer, L.P. Mikkelsen, L.E. Asp, B.J. Blinzler, Automated X-ray computer tomography segmentation method for finite element analysis of non-crimp fabric reinforced composites, *Compos. Struct.* 256 (2021) 113136, doi:[10.1016/j.compstruct.2020.113136](#).
- [2] R.M. Auenhammer, Lars P. Mikkelsen, Leif E. Asp, Brina J. Blinzler, X-ray tomography based numerical analysis of stress concentrations in non-crimp fabric reinforced composites - assessment of segmentation methods. *IOP Conference Ser.*, 942, 012038. doi: [10.1088/1757-899X/942/1/012038](#).
- [3] K.M. Jespersen, J. Zangenberg, T. Lowe, P.J. Withers, L.P. Mikkelsen, Fatigue damage assessment of uni-directional non-crimp fabric reinforced polyester composite using X-ray computed tomography, *Compos. Sci. Technol.* 136 (2016) 94–103, doi:[10.1016/j.compscitech.2016.10.006](#).
- [4] K.M. Jespersen, J.A. Glud, J. Zangenberg, A. Hosoi, H. Kawada, L.P. Mikkelsen, Uncovering the fatigue damage initiation and progression in uni-directional non-crimp fabric reinforced polyester composite, *Composites, Part A* 109 (2018) 481–497, doi:[10.1016/j.compositesa.2018.03.002](#).